

PAPER

Low-Complexity Hybrid Precoding Based on PAST for Millimeter Wave Massive MIMO System

Rui JIANG[†], Xiao ZHOU[†], You Yun XU^{†a)}, and Li ZHANG^{††}, *Nonmembers*

SUMMARY Millimeter wave (mmWave) massive Multiple-Input Multiple-Output (MIMO) systems generally adopt hybrid precoding combining digital and analog precoder as an alternative to full digital precoding to reduce RF chains and energy consumption. In order to balance the relationship between spectral efficiency, energy efficiency and hardware complexity, the hybrid-connected system structure should be adopted, and then the solution process of hybrid precoding can be simplified by decomposing the total achievable rate into several sub-rates. However, the singular value decomposition (SVD) incurs high complexity in calculating the optimal unconstrained hybrid precoder for each sub-rate. Therefore, this paper proposes PAST, a low complexity hybrid precoding algorithm based on projection approximate subspace tracking. The optimal unconstrained hybrid precoder of each sub-rate is estimated with the PAST algorithm, which avoids the high complexity process of calculating the left and right singular vectors and singular value matrix by SVD. Simulations demonstrate that PAST matches the spectral efficiency of SVD-based hybrid precoding in full-connected (FC), hybrid-connected (HC) and sub-connected (SC) system structure. Moreover, the superiority of PAST over SVD-based hybrid precoding in terms of complexity and increases with the number of transmitting antennas.

key words: massive multiple-input multiple-output (MIMO), millimeter wave (mmWave) communication, hybrid precoding, singular value decomposition (SVD), projection approximate subspace tracking (PAST)

1. Introduction

In order to meet the rapid growing in mobile data traffic on wireless communication, Millimeter wave (mmWave) communication, which provides rich spectrum resource and high data transmission rate, can effectively enhance Internet capacity of communication system [1], [2]. However, in the mmWave bands, 30 GHz to 300 GHz, radio communication suffers huge path loss [3], which significantly decreases communication quality. Fortunately, the short wavelength of 1 mm to 10 mm makes it possible to pack dozens or even hundreds of antennas into a small device [4]. Therefore, mmWave system can leverage massive Multiple-Input Multiple-Output (MIMO) antenna array to compensate the free space path loss of mmWave signals with beamforming gain.

In traditional MIMO systems, the data streams are pre-

coded in full digital precoding to eliminate interference and then transmitted through the radio frequency (RF) chain to the transmitting antenna. The full digital precoding, which can control the amplitude and phase of the signal simultaneously, could achieve high multiplexing gain and anticipant system performance. However, as each antenna in the full digital precoding is connected to an RF chain, the hundreds of antennas in massive MIMO system need to configure hundreds of RF chains. The high energy consumption and implementation cost caused by RF chains make it prohibitive to implement full digital precoding [5], [6]. Hence, hybrid precoding structure is proposed. In this structure, the data streams are first pre-coded in digital precoding, and traverse RF chains, which are connected with antennas through phase shifters. Then, the data streams are pre-coded in the analog precoder composed by phase shifters. It can reduce RF chains and energy consumption significantly [7], [8].

In general, the hybrid precoding structure is divided into two categories: full-connected (FC) structure and sub-connected (SC) structure. In the FC structure, each RF chain is connected to all antennas through phase shifters, which can achieve high spectral efficiency [8]–[12]. However, if base station terminal hosts hundreds or thousands of antennas because of the large-scale application of MIMO, the phase shifters in the FC structure will also increase greatly, which will still result in the significant energy consumption and hardware complexity. To avoid this problem, the SC structure makes each RF chain connect to part of antennas through phase shifters which greatly reduces the number of phase shifters needed [13]–[16]. Although the phase shifters are reduced observably in SC structure, its spectral efficiency is lower than FC structure. Hence, hybrid connected (HC) structure is proposed to balance the spectral efficiency, energy consumption and hardware complexity of FC and SC structure [17]–[20]. In HC structure, all antennas and RF chains are divided into several subarrays, in which each RF chain is connected with all antennas through phase shifters, which reduces phase shifters compared with FC and improves spectral efficiency compared with SC structure significantly.

According to the structure of mmWave channel, the idea of spatial constraint matrix reconstruction is applied to the solution of analog and digital precoder by using orthogonal matching pursuit (OMP) algorithm, so as to achieve near-optimal spectral efficiency [8]. Due to the high complexity of OMP algorithm, the alternate minimization algorithm was proposed in [8] through imposing orthogonal

Manuscript received November 15, 2021.

Manuscript revised March 2, 2022.

Manuscript publicized April 21, 2022.

[†]The authors are with College of Telecommunications and Information Engineering and National Engineering Research Center of Communications and Networking, Nanjing University of Posts and Telecommunications, Nanjing 210003, China.

^{††}The author is with College of Computer, Nanjing Forestry University, Nanjing 210037, China.

a) E-mail: yyxu@njupt.edu.cn

DOI: 10.1587/transcom.2021EBP3188

constraints on the digital precoder, which is low complexity. This method could optimize alternately the digital and analog precoder in each iteration. However, the above two algorithms are aimed at FC system structure, which will lead to high hardware complexity and energy consumption. The SC system structure is adopted in [13], which applies an idea of the successive interference elimination (SIC) to the process of solving digital and analog precoding. In this method, the complex total achievable rate is decomposed into several sub-rates, which can be optimized successively. Nevertheless, compared with FC structure, the spectral efficiency in [13] is lower. Therefore, a hybrid precoding algorithm based on singular value decomposition (SVD) for HC structure is proposed in [19]. It calculates optimal unconstrained hybrid precoding matrix by utilizing SVD and gets hybrid precoding with constraint conditions. The spectrum efficiency of the SVD-based hybrid precoding is near that of the optimal unconstrained hybrid precoding. However, with the increase of antennas at the transmitter, the dimensions of the matrix to perform SVD also increase, which makes SVD process more complex and time-consuming.

To sum up, aiming at the high complexity brought by SVD in calculating the optimal unconstrained hybrid precoding matrix, we investigate the hybrid precoding scheme for HC structure. Firstly, the total achievable rate is simplified into several sub-rates, which are maximized by using SIC idea. Then, a low complexity hybrid precoding algorithm based on projection approximation subspace tracking (PAST) is proposed for each sub-rate optimization process. It has a lower complexity for avoiding the SVD process in calculating the optimal unconstrained hybrid precoding for each sub-rate. Simulation results show that the proposed algorithm can achieve almost the same performance as the hybrid precoding based on SVD in HC system architecture. And with the increase of transmitting antennas, the time consumption and complexity of the proposed algorithm are much lower than that of the SVD-based hybrid precoding, which can meet the real-time processing requirements of the communication. Moreover, the proposed algorithm has good universality, which can be applied to FC, SC and HC systems.

Notation: A^T , A^H , A^* , A^{-1} , $|A|$, $\|A\|_F$ denote the transpose, conjugate transpose, complex conjugation, inversion, determinant and Frobenius norm of matrix A , respectively; $E[\cdot]$ represents mathematical expectation and I_N represents a $N \times N$ identity matrix. The $CN(\mu, \sigma^2)$ denotes complex Gaussian distribution with mean μ and variance σ^2 .

2. System Model

The transmitter is equipped with N_t antennas and N_{RF} RF chains in HC structure as shown in Fig. 1. The antennas and RF chains at the transmitter are divided into D sub-arrays, in which there is K (N_{RF}/D) RF chains connected with T (N_t/D) antennas through phase shifters. The N_s data streams pass through the RF chains after being pre-coded by the digital precoder $F_{BB} \in \mathbb{C}^{N_{RF} \times N_s}$, to be pre-coded in the

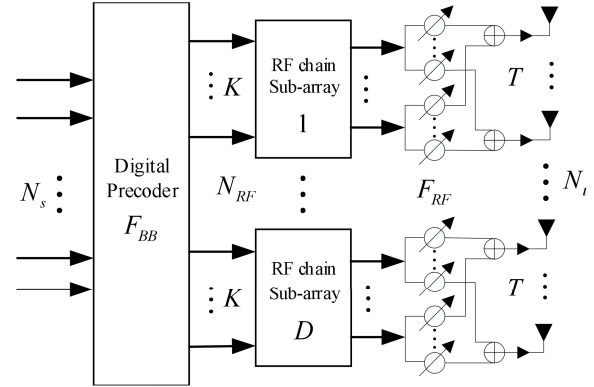


Fig. 1 The hybrid precoding system architecture for HC structure.

analog precoder $F_{RF} \in \mathbb{C}^{N_t \times N_{RF}}$ and finally sent to the antennas at the transmitter, where N_{RF} is subject to constraint $N_s \leq N_{RF} \leq N_t$. Thus, when the receiver is equipped with N_r antennas, the received signal $y \in \mathbb{C}^{N_r \times 1}$ can be expressed as:

$$y = \sqrt{\rho} H F_{RF} F_{BB} s + n = \sqrt{\rho} H F s + n \quad (1)$$

Where, ρ represents for the average received power; $H \in \mathbb{C}^{N_r \times N_t}$ is the channel matrix; s is the $N_s \times 1$ signal vector satisfied to $E[ss^H] = \frac{1}{N_s} I_{N_s}$, where $E[\cdot]$ represents mathematical expectation; n is the additive white Gaussian noise vector, and obeys $n \in CN(0, \sigma^2)$.

The received signal y will be processed in the combiner W , then we have:

$$\tilde{y} = \sqrt{\rho} W^H H F s + W^H n \quad (2)$$

When signals are transmitted through the millimeter wave channel, the spectral efficiency of the system is [8]:

$$R = \log_2 \left(\left| I_{N_s} + \frac{\rho}{N_s} R_n^{-1} W^H H F_{RF} F_{BB} F_{BB}^H F_{RF}^H H^H W \right| \right) \quad (3)$$

Where, $R_n = \sigma^2 W^H W$ represents the noise covariance matrix after combining.

The hybrid precoding matrix F with $N_t \times N_s$ dimension is a combination of analog and digital precoding matrices. Since divided into several mutually independent submatrices according to structure of HC, the analog precoder is a block diagonal matrix, which can be expressed as:

$$F_{RF} = \begin{bmatrix} F_{RF,1} & & \\ & \ddots & \\ & & F_{RF,D} \end{bmatrix} \quad (4)$$

where, the dimension of each submatrix of the analog precoding matrix is $T \times K$. In the i th submatrix with $F_{RF,i} = [a_{i,1}, a_{i,2}, \dots, a_{i,K}]$, the dimension of analog precoding vector $a_{i,j}$ corresponding to the j th RF chain is $T \times 1$. All non-zero elements of $F_{RF,i}$ should satisfy the identity amplitude constraint, but with different phases, namely $|F_{RF,i}(\cdot, \cdot)| =$

$1/\sqrt{T}$. Meanwhile, considering the complexity of the precoding design and the simplification of the following optimization objective, it is assumed that the digital precoding matrix is also a block diagonal matrix, given by:

$$F_{BB} = \begin{bmatrix} F_{BB,1} & & \\ & \ddots & \\ & & F_{BB,D} \end{bmatrix} \quad (5)$$

The digital precoding matrix of each submatrix is $K \times K$ dimension, provided $N_{RF} = N_s$. $F_{BB,i} = [b_{i,1}; b_{i,2}; \dots; b_{i,K}]$ and $b_{i,j}$ is a digital precoding vector with $1 \times K$ dimension. Hence, the hybrid precoding matrix is also a block diagonal matrix meeting the total transmitted power constraint $\|F_{RF}F_{BB}\|_F^2 \leq N_s$.

Due to the characteristic of free-space pathloss in mmWave communication, the transmission path of the mmWave signal is few and sparse. The traditional MIMO channel modeling methods are not suitable for channel models because of the limited scattering of mmWave channels. Therefore, the extended Saleh-Valenzuela cluster channel model is adopted in this paper, which depicts the channel matrix H as

$$H = \sqrt{\frac{N_t N_r}{N_{cl} N_{ray}}} \sum_{i=1}^{N_{cl}} \sum_{j=1}^{N_{ray}} \alpha_{ij} \cdot \mathbf{a}_r(\varphi_{ij}^r, \theta_{ij}^r) \cdot \mathbf{a}_t(\varphi_{ij}^t, \theta_{ij}^t)^H \quad (6)$$

Where N_{cl} and N_{ray} represent channel scattering clusters and propagation paths in each scattering cluster respectively. In the j th propagation path of the i th scattering cluster, α_{ij} stands for the gain in propagation path characterizing independently and identically distributed $CN(0, \sigma_{\alpha_{ij}})$. φ_{ij}^t and θ_{ij}^t represent the azimuth and elevation angle of departure; φ_{ij}^r and θ_{ij}^r represent the azimuth and elevation angle of arrival. $\mathbf{a}_r(\varphi_{ij}^r, \theta_{ij}^r)$ and $\mathbf{a}_t(\varphi_{ij}^t, \theta_{ij}^t)$ denote the normalized array response vectors at the receiver and transmitter. When the uniform planar array (UPA) is considered to applied at the transceiver, $\mathbf{a}_r(\varphi_{ij}^r, \theta_{ij}^r)$ and $\mathbf{a}_t(\varphi_{ij}^t, \theta_{ij}^t)$ can be written as

$$\mathbf{a}_{r/t}(\varphi, \theta) = \frac{1}{\sqrt{N_{r/t}}} \left[1, \dots, e^{j\frac{2\pi}{\lambda}d(m \sin \varphi \sin \theta + n \cos \theta)}, \dots, e^{j\frac{2\pi}{\lambda}d((M-1) \sin \varphi \sin \theta + (N-1) \cos \theta)} \right]^T \quad (7)$$

Where $N_{r/t}$ is antennas at the receiver or transmitter; d and λ are the space between antenna units and wavelength; M and N meet the equation of $N_{r/t} = M \cdot N$, and $0 \leq m < M$, $0 \leq n < N$.

3. A Hybrid Precoding Based on PAST for HC System Structure

In this section, the total achievable rate for HC system structure is decomposed into several sub-rate issues optimized via SIC idea. Then, the optimal unconstrained hybrid precoding of each sub-array is estimated by leveraging the PAST algorithm. The hybrid precoding with constraints is

finally obtained.

3.1 Decomposition of the Optimization Problem

According to [8], in order to simplify the design of the precoding and combining matrix, the joint optimization problem (3) is decoupled, and the design of the precoding is mainly studied. In HC system, the total achievable rate R is stated as

$$R = \log_2 \left(\left| I_{N_r} + \frac{\rho}{N_s \sigma^2} H F F^H H^H \right| \right) \quad (8)$$

The optimization objective is to maximize the achievable rate by designing a hybrid precoding matrix F , and the objective function is

$$\begin{aligned} F^{opt} &= \arg \max_F \log_2 \left(\left| I_{N_r} + \frac{\rho}{N_s \sigma^2} H F F^H H^H \right| \right) \\ \text{s.t. } & |F_{RF,i}(\cdot, \cdot)| = 1/\sqrt{T} \\ & \|F\|_F^2 = \|F_{RF}F_{BB}\|_F^2 \leq N_s \end{aligned} \quad (9)$$

Unfortunately, the non-convex constraints of the formula (9), namely the constraints of total transmitted power on the hybrid precoder and identical amplitude over all non-zero elements in analog precoder, make it difficult to solve the objective function (9). Consider that the hybrid precoding matrix F has a characteristic of is a block diagonalization, where the precoding of each submatrix is independent of each other, then there is

$$F = F_{RF}F_{BB} = \text{diag} \{ F_{RF,1}F_{BB,1}, \dots, F_{RF,D}F_{BB,D} \} \quad (10)$$

Therefore, the R can be decomposed into multiple sub-rate optimization problems, and the optimal solution of the objective function (9) can be obtained by maximizing the corresponding sub-rate of each sub-array.

According to the structure of the hybrid precoding matrix, the matrix F is divided into D submatrices, i.e., $F = [f_1, f_2, \dots, f_D]$. It is further expressed as $F = [F_{D-1} f_D]$, where $F_{D-1} \in \mathbb{C}^{N_r \times K(D-1)}$ represents the first $D-1$ submatrices and $f_D \in \mathbb{C}^{N_r \times K}$ is the D th submatrix. Hence, the total achievable rate in formula (8) can be rewritten as

$$\begin{aligned} R &= \log_2 \left(\left| I_{N_r} + \frac{\rho}{N_s \sigma^2} H F F^H H^H \right| \right) \\ &= \log_2 \left(\left| I_{N_r} + \frac{\rho}{N_s \sigma^2} H [F_{D-1} f_D] [F_{D-1} f_D]^H H^H \right| \right) \\ &= \log_2 \left(\left| I_{N_r} + \frac{\rho}{N_s \sigma^2} (H F_{D-1} F_{D-1}^H H^H + H f_D f_D^H H^H) \right| \right) \\ &\stackrel{(a)}{=} \log_2 (|Q_{D-1}|) + \log_2 \left(\left| I_{N_r} + \frac{\rho}{N_s \sigma^2} Q_{D-1}^{-1} H f_D f_D^H H^H \right| \right) \quad (11) \\ &\vdots \\ &\stackrel{(b)}{=} \sum_{i=1}^D \log_2 \left(\left| I_{N_r} + \frac{\rho}{N_s \sigma^2} Q_{i-1}^{-1} H f_i f_i^H H^H \right| \right) \end{aligned}$$

$$\stackrel{(c)}{=} \sum_{i=1}^D \log_2 \left(\left| I_K + \frac{\rho}{N_s \sigma^2} f_i^H H^H Q_{i-1}^{-1} H f_i \right| \right)$$

Where (a) can be obtained on the basis of the fact that $|AB| = |A| \cdot |B|$, and the defined auxiliary matrix $Q_{D-1} = I_{N_r} + \frac{\rho}{N_s \sigma^2} H F_{D-1} F_{D-1}^H H^H$. Since $\log_2(|Q_{D-1}|)$ has the same form as Eq. (8), matrix Q_{D-1} can be further decomposed in the similar method, as detailed in Appendix A. When the total achievable rate formula is fully decomposed, the result of (b) is acquired. Finally, transform the form of formula according to the principle $|I + AB| = |I + BA|$ defining $A = Q_{i-1}^{-1} H f_i$ and $B = f_i^H H^H$ to obtain (c), where $Q_i = I_K + \frac{\rho}{N_s \sigma^2} H F_i F_i^H H^H$ and $Q_0 = I_K$.

It can be seen from Eq. (11) that the total achievable rate is finally decomposed into multiple sub-rates. According to the SIC idea for multi-user signal detection mentioned in [13], which refers to removing the signal interference of other $k - 1$ users when the receiver detects the signal of the k th user, the sub-rate of the first subarray is optimized to obtain the hybrid precoding matrix f_1 . The matrix F_1 formed by f_1 is used to update the auxiliary matrix Q_1^{-1} . It can be utilized to eliminate the interference of the first subarray on the second subarray, and then the sub-rate of the second subarray could be optimized to obtain the hybrid precoding matrix f_2 . The matrix F_2 formed by f_1 and f_2 is used to update the auxiliary matrix Q_2^{-1} , which will be utilized to eliminate the interference of the first and second subarray on the third subarray f_3 . In a similar way, the hybrid precoding matrix of all subarrays can be obtained.

3.2 Design of Hybrid Precoding Matrices with Constraints

According to (11), the sub-rate optimization problem of the i th subarray can be stated as

$$f_i^{opt} = \arg \max_{f_i \in \mathbb{F}} \log_2 \left(\left| I_K + \frac{\rho}{N_s \sigma^2} f_i^H P_{i-1} f_i \right| \right) \quad (12)$$

Where \mathbb{F} is all set of hybrid precoding matrices satisfying the constraints described in (9), and $P_{i-1} = H^H Q_{i-1}^{-1} H$ is a $N_t \times N_t$ Hermitian matrix. It is can realized from (10) that the hybrid precoding of HC structure is block diagonal matrix, in which non-zero elements in the i th precoding matrix f_i is from $((i-1)T + 1)$ to iT rows. Therefore, (12) can be further written as

$$\widehat{f}_i^{opt} = \arg \max_{\widehat{f}_i \in \widehat{\mathbb{F}}} \log_2 \left(\left| I_K + \frac{\rho}{N_s \sigma^2} \widehat{f}_i^H \widehat{P}_{i-1} \widehat{f}_i \right| \right) \quad (13)$$

Similarly, $\widehat{\mathbb{F}}$ is a feasible set of $T \times K$ dimensionality that satisfies the constraints and \widehat{P}_{i-1} is a submatrix cut off from $((i-1)T + 1)$ to iT rows and columns of P_{i-1} , which is $T \times T$ Hermitian matrix.

SVD of \widehat{P}_{i-1} is performed, that is, $\widehat{P}_{i-1} = V \Sigma V^H$, where Σ is a $T \times T$ diagonal matrix, elements of which are singular value of \widehat{P}_{i-1} and arranged from largest to smallest, and V is the $T \times T$ unitary matrix. The optimal unconstrained hybrid

precoding of the i th subarray in (13), denoted as V_K , is the first K column of right singular matrix V of \widehat{P}_{i-1} , namely

$$\widehat{f}_i^{opt} = V(:, 1 : K) = V_K \quad (14)$$

Then, the optimal unconstrained hybrid precoding of the $i + 1$ th subarray is obtained in the same SVD method according to \widehat{P}_i updated by V_K of the i th subarray. Finally, the total optimal unconstrained hybrid precoding matrix F^{opt} can be get. However, F^{opt} is not a final hybrid precoding matrix due to constraints described in (9). Therefore, we obtain the corresponding hybrid precoding matrix of each subarray from the feasible set under the constraints.

According to [8], optimization problem (13) can be equivalent to the following formula

$$\widehat{f}_i^{opt} = \arg \min_{\widehat{f}_i \in \widehat{\mathbb{F}}} \|V_K - \widehat{f}_i\|_F^2 \quad (15)$$

Proof: See Appendix B.

The hybrid precoding matrix can be obtained by minimizing the Euclidean distance with V_K .

Using the phase extraction method to satisfy the identity amplitude constraint, analog precoding matrix is optimized as

$$F_{RF,i} = \frac{1}{\sqrt{T}} \exp(j * \text{angle}(V_K)) \quad (16)$$

When $K = 1$, that is, there is only one RF chain of the subarray, the digital precoding and the final obtained hybrid precoding matrix are as follows:

$$F_{BB,i} = \frac{1}{\sqrt{T}} \|V_K\|_1 \quad (17)$$

$$\widehat{f}_i = \frac{1}{T} \|V_K\|_1 \exp(j * \text{angle}(V_K)) \quad (18)$$

When $K > 1$, namely the RF chain of the subarray is greater than 1, the digital precoding is solved by the least square method, and the final precoding matrix is obtained as follows:

$$F_{BB,i} = (F_{RF,i}^H F_{RF,i})^{-1} F_{RF,i}^H V_K \quad (19)$$

$$\widehat{f}_i = F_{RF,i} F_{BB,i} \quad (20)$$

All the sub-rate optimization problems are solved by the same method to acquire the hybrid precoding matrix with the constraints.

3.3 The Hybrid Precoding Based on PAST Algorithm

In formula (14), SVD is performed on the auxiliary matrix \widehat{P}_{i-1} , and the first K columns of the right singular matrix of \widehat{P}_{i-1} is selected as the optimal unconstrained hybrid precoding matrix \widehat{f}_i^{opt} of the i th subarray. However, as antennas increases, the dimensions of the matrix \widehat{P}_{i-1} will gradually increase, which will result in a high complexity and time

consumption of SVD for \widehat{P}_{i-1} . Therefore, the PAST algorithm with a lower complexity is adopted to estimate only the required major column vectors of the right singular matrix to avoid the SVD process of calculating the whole right singular matrix.

In the PAST algorithm, we will take $PP = \widehat{P}_{i-1}^H \widehat{P}_{i-1}$ as the data sample matrix, row of which is considered as the data sample vector x . When the data sample vector x_j is input to estimate value of the most dominant singular vector w_j of the matrix \widehat{P}_{i-1} , the PAST algorithm can be simplified as

$$w_j = w_{j-1} + \frac{1}{d_j} [x_j - w_{j-1}y_j] y_j^* \quad (21)$$

Where $y_j = w_j^H x_j$ and $d_j = d_{j-1} + |y_j|^2$. It can be seen that the PAST algorithm is a gradient algorithm whose step size d_j is used for self-tuning. The projection of the current data sample vector x_j on w_j is removed from x_j itself after the most dominant singular vector w_j is estimated. At this point, the second dominant singular vector dominates the estimation vector to be updated, which can be estimated and extracted just like the most dominant singular vector. The process is repeated until all the singular vectors W_j are estimated in order.

Then, continue to input the data sample vectors x_{j+1} and update all the singular vectors W_{j+1} in order by (21) combining with the estimated value W_j of the singular vectors obtained in the previous process, until all the data sample vectors participate in the estimation. The PAST is an estimation algorithm, and leads to the loss of orthogonality between the columns of the final estimation result W_T . Hence, orthogonalization processing of W_T is required at the end of the algorithm. In the simulation, orthogonalization is realized by function `orth()` in MATLAB. The singular vector estimation process for the auxiliary matrix \widehat{P}_{i-1} is shown in algorithm 1.

Based on the above analysis, the algorithm in this paper first calculates the estimated value V_K of the first K columns of the right singular matrix for the auxiliary matrix \widehat{P} according to algorithm 1, and then utilizes V_K to achieve $F_{RF,i}$, $F_{BB,i}$ and hybrid precoding matrix under the constraints. The methods of solving the digital precoding matrix are different according to RF chains in subarray. Then, the matrix F of the whole system is formed diagonally by that of subarrays. Finally, the updated results for \widehat{P} through the obtained subarray hybrid precoding matrix are used as the input of the next subarray hybrid precoding solution. When all the submatrix hybrid precoding matrices have been calculated, the block diagonal-form hybrid precoding matrix F of the whole system is output. The specific algorithm flow is shown in algorithm 2.

Algorithm 1: Projection approximation subspace tracking (PAST) algorithm.

Input: auxiliary matrix \widehat{P}_{i-1} , the number K of singular vectors to be estimated.

Output: The estimation V_K of the first K columns of the

right singular matrix of the auxiliary matrix \widehat{P}_{i-1} .

Initialization: W_0, d_0

1. $PP = \widehat{P}_{i-1}^H \widehat{P}_{i-1}$
2. *for* $j = 1 : T$
3. $x_j = PP^H(j, :)$
4. *for* $k = 1 : K$
5. $y = W_{j-1}^H(:, k) \cdot x_j$
6. $d_j(k) = d_{j-1}(k) + |y|^2$
7. $e = x_j - W_{j-1}(:, k) \cdot y$
8. $W_j(:, k) = W_{j-1}(:, k) + e \cdot y^* / d_j(k)$
9. $x_j = x_j - W_j(:, k) \cdot y$
10. *end for*
11. *end for*
12. $V_K = \text{orth}(W_T)$

Algorithm 2: The hybrid precoding based on PAST algorithm

Input: channel matrix H, D, K .

Output: The hybrid precoding matrix F .

1. $P_0 = H^H H$
2. *for* $i = 1 : D$
3. $\widehat{P}_{i-1} = V \Sigma V^H$ obtained by algorithm 1
4. $F_{RF,i} = \frac{1}{\sqrt{T}} \exp(j * \text{angle}(V_K))$
5. *if* $K = 1$
6. $F_{BB,i} = \frac{1}{\sqrt{T}} \|V_K\|_1$
7. *else*
8. $F_{BB,i} = (F_{RF,i}^H F_{RF,i})^{-1} F_{RF,i}^H V_K$
9. *end if*
10. $\widehat{f}_i = F_{RF,i} F_{BB,i}$
11. $F = \text{blkdiag}[F, \widehat{f}_i]$
12. $Q_i = I_{N_r} + \frac{\rho}{N_s \sigma^2} H F_i F_i^H H^H$
13. $P_i = H^H Q_i^{-1} H$
14. *end for*

It is worth mentioning that the proposed PAST-based hybrid precoding can be also applied to the combining at the user following the similar method in [8] after the hybrid precoding matrix F is designed. Similar to [13], the research in this paper only focuses on hybrid precoding and further discussion about hybrid combining will be left for future work.

4. Simulation Results

In this section, we consider the optimal unconstrained hybrid precoding FC-OPT in the FC system structure, the OMP algorithm FC-OMP in [8], the Power Iteration (PI) algorithm SC-PI in [13] and the SVD algorithm for connection modes of FC, HC and SC in [19] as comparison to demonstrate performance of the proposed algorithm in the simulation experiment. In the simulation experiment, the parameters of hybrid precoding system architecture are set as follow: $N_t = 144$, $N_r = 36$ and $N_s = N_{RF}$. In particular, HC system structure is divided into two subarrays, namely $D = 2$. The distance between the antenna units $d = \frac{\lambda}{2}$ and Signal-to-noise Ratio (SNR) is defined as $\frac{\rho}{\sigma^2}$.

The mmWave channel strictly decides the spectral efficiency of hybrid precoding algorithm. Therefore, the influence of the scattering clusters of mmWave channel pa-

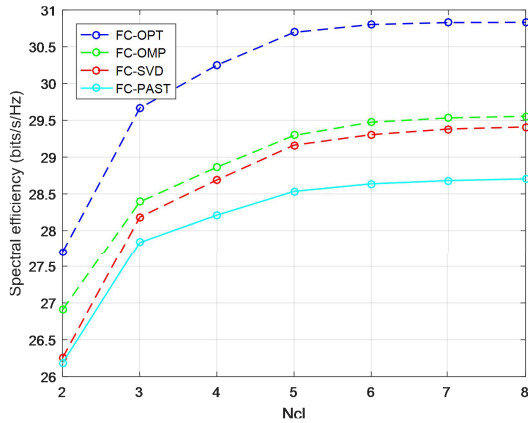


Fig. 2 Spectrum efficiency of the hybrid precoding algorithms with different scattering clusters.

parameter on the spectral efficiency of hybrid precoding with FC structure at $SNR = 0$ dB is illustrated. As can be seen in Fig. 2, with the increase of number of scattering clusters N_{cl} , the spectral efficiency of each hybrid precoding gradually increases, which is due to the increase of signal transmission paths. When $N_{cl} \geq 5$, the spectral efficiency is basically stable. Therefore, the number of scattering clusters N_{cl} is set to 5. The number of propagation paths N_{ray} is usually set to 10. To reduce interference and increase beamforming gain, the directional and omnidirectional antenna array are used in the transmitter and receiver, respectively. Similar to [8], The azimuth and elevation widths of the transmitting end are 60° and 20° respectively. Hence, The parameters φ_{ij}^t and θ_{ij}^t in transmitter are assumed to follow a uniform distribution within $[-30^\circ, 30^\circ]$ and $[70^\circ, 90^\circ]$; φ_{ij}^r and θ_{ij}^r of receiver are uniformly distribute in $[-180^\circ, 180^\circ]$ and $[0, 180^\circ]$ respectively. In particular, a scattering cluster of azimuth of departure is formed by taking an angle between -30° and 30° based on the uniform distribution, and then doing angular spread of 7.5° . In the cluster, the specific angle of each propagation path is obtained according to the uniform distribution.

Figure 3 shows the spectral efficiency comparison of hybrid precoding algorithms, where $N_s = N_{RF} = 4$. The calculation of spectral efficiency is shown in (3). However, since the combiner is not studied in this paper, the optimal combiner matrix is used to calculate the spectral efficiency of the schemes, namely $W_{opt} = U(:, 1 : N_s)$ and $H = U\Sigma V^H$. Firstly, the PAST-based hybrid precoding proposed in this paper is simulated in FC, SC and HC system structures. We can observe from Fig. 3 that the proposed PAST-based hybrid precoding schemes is applicable for FC, SC and HC structure by setting the number of system structure subarrays as $D = 1$, $D = 2$ and $D = 4$ respectively. The PAST-based hybrid precoding for HC structure is the focus of this paper. When comparing the spectral efficiency of the algorithms, only the algorithms under the same system connection structure is compared, and no comparison is made between algorithms with different connection structure. In

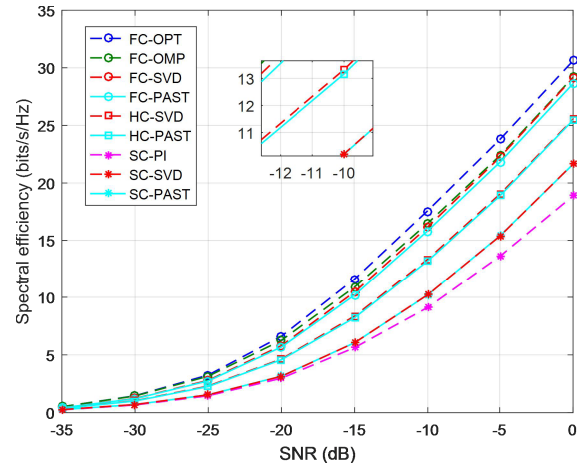


Fig. 3 Spectrum efficiency of the hybrid precoding algorithms.

FC structure, FC-OPT is the optimal unconstrained hybrid precoding algorithm, and its spectral efficiency is the highest; meanwhile, the spectral efficiency of the proposed algorithm FC-PAST is close to that of FC-SVD and FC-OMP. In HC structure, the proposed algorithm HC-PAST can achieve approximate spectral efficiency as HC-SVD. In the SC structure, the spectral efficiency of the proposed SC-PAST algorithm is almost the same as that of SC-SVD, but higher than that of SC-PI algorithm. To sum up, the proposed algorithm can achieve high spectral efficiency and has the performance close to the SVD-based hybrid precoding.

Figure 4 provides the comparison of the spectral efficiencies of hybrid precoding schemes under different RF chains at $SNR = 0$ dB and $SNR = -10$ dB. Figure 4 further illustrates the spectral efficiency of the proposed algorithm from the perspective of the RF chain. As can be seen from the Fig. 4, no matter how RF chains changes, the proposed PAST-based hybrid precoding schemes can achieve close spectral efficiency as SVD-based in the same connection structure. In particular, the proposed SC-PAST algorithm always achieves higher spectral efficiency than SC-PI. Therefore, the proposed algorithm in this paper still has good performance when the RF chain changes. Combined with Fig. 3, we further find that the FC structure achieves greater spectral efficiency than HC, and similarly the HC is greater than SC. Therefore, the HC structure achieves much better balance of the spectral efficiency between FC and SC structure. However, the spectral efficiency of some algorithms in Fig. 4 are likely to reduce with the increase of RF chains. This is because when the total power of the transmission is limited and equal power allocation is hypothesized, the increase of data streams N_s will result in a reduction in the average power allocated to each data stream. In particular, in the SC structure the digital precoding is a diagonal matrix as RF chain of each subarray is one, which only has a function of power allocation and does not eliminate the interference between the data streams. Therefore, the spectral efficiency possibly decreases as the RF chains increase. Meanwhile, by further comparison of Figs. 4(a)

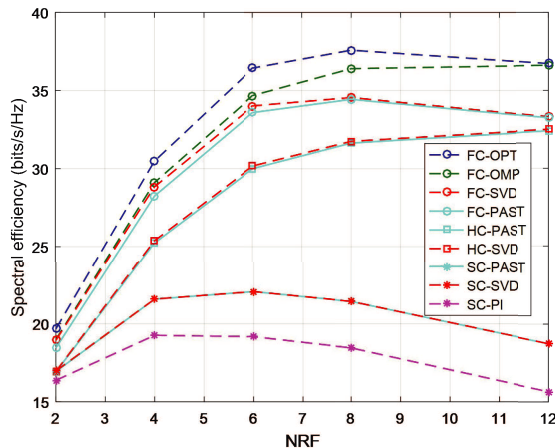
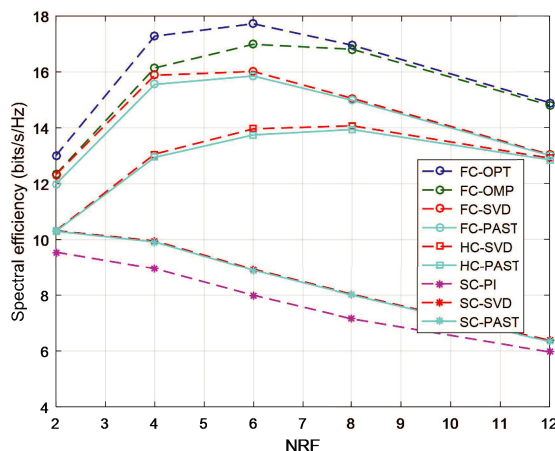
(a) Spectrum efficiency at $SNR = 0dB$ (b) Spectrum efficiency at $SNR = -10dB$

Fig. 4 Spectrum efficiency of the hybrid precoding algorithm with different RF chains.

and 4(b), it can be seen that the overall spectral efficiency of hybrid precoding algorithm is higher when $SNR = 0dB$. This is because the interference of the noise to the signal is small when the SNR is high, so the system achievable performance of both the proposed and other algorithms is better.

The energy efficiency comparison of HC-PAST, FC-OMP and SC-PI hybrid precoding schemes at $SNR = 0dB$ and $SNR = -10dB$ is showed in Fig. 5. Since the energy efficiency is related to the connection structure of the system, the PAST-based algorithm for HC structure is selected for comparison with the algorithms corresponding to FC and SC structure. The energy efficiency η is the ratio of spectral efficiency R to the total power consumption of the system, namely:

$$\eta = \frac{R}{P_t + N_t P_{PA} + N_{RF} P_{RF} + N_{PS} P_{PS}} \quad (22)$$

Where P_t is the energy of the transmitter; P_{PA} is the energy consumed by the power amplifier at the antenna transmitter;

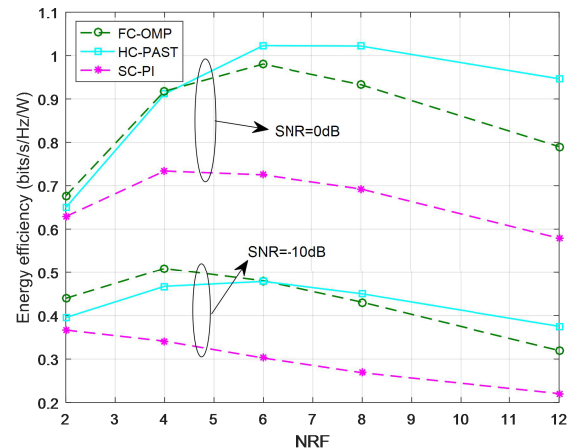


Fig. 5 Energy efficiency of hybrid precoding algorithm with different RF chains.

P_{RF} and P_{PS} are the energy consumed by each RF chain, and phase shifter, respectively and N_{PS} represents the total phase shifters of system. The power consumption of each component is set as: $P_t = 10W$, $P_{PA} = 100mW$, $P_{RF} = 100mW$, $P_{PS} = 10mW$. In simulation, the total transmitting antennas N_t , RF chains N_{RF} and transmitter energy P_t are set to same values in the different hybrid precoding schemes. The differences between hybrid precoding schemes are the number of phase shifters and the spectral efficiency. It can be seen from Fig. 4 that HC-PAST can achieve relatively high spectral efficiency. Meanwhile, the number of phase shifters N_{PS} in FC-OMP and SC structure are $N_{RF} \times N_t$ and N_t respectively, and N_{PS} in HC-PAST is 1/4 of that in FC-OMP. Hence, the low number of phase shifters and the high spectral efficiency are the main reason for the energy efficiency of HC over 1.0 at $SNR = 0dB$ when RF chains is 6 or 8 in Fig. 5. On the other hand, it can be seen from Figure 4 that the spectral efficiency of the hybrid precoding algorithms is generally very low when $SNR = -10dB$. It results in lower energy efficiency of the hybrid precoding algorithms in Fig. 5. Therefore, the low spectral efficiency makes the energy efficiency of the hybrid precoding algorithms insufficient to exceed 1.0. We could observe from Figure 5 that the energy efficiency of the HC-PAST scheme is always higher than the SC-PI scheme. When RF chains is 2 or 4 at $SNR = 0dB$, the energy efficiency of HC-PAST is close to that of FC-OMP; when RF chains is greater than 6, the energy efficiency of HC-PAST is higher than that of FC-OMP. Therefore, HC-PAST with high energy efficiency achieves trade-off of the hardware complexity and spectral efficiency between FC-OMP and SC-PI.

Figure 6 provides the time consumption comparison between SVD and the PAST algorithm at $SNR = 0dB$ and $N_s = N_{RF} = 4$. The time consumption is obtained with Matlab on a PC of 1.60 GHz. It can be observed from Fig. 6 that the HC-PAST consumes slightly more time than HC-SVD in $N_t \leq 256$. The time consumed by both HC-SVD and SVD is much higher than that of HC-PAST and PAST in $N_t > 256$, respectively, and with the increase of N_t , the

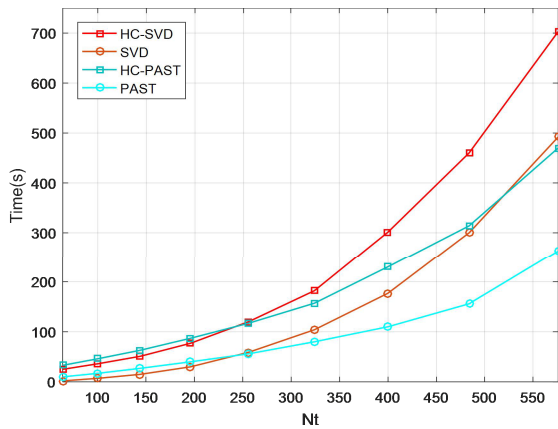


Fig. 6 Time consumption of algorithm with different transmitting antennas.

time consumption of SVD is almost twice that of PAST algorithm. According to [21], calculating a right singular matrix of $m \times n$ matrix \hat{P}_{i-1} with SVD requires at least $n^2 + O(n^3)$ operations, where mn^2 is complexity of calculating $\hat{P}_{i-1}^H \hat{P}_{i-1}$. When estimating the first K columns of a right singular matrix of $m \times n$ matrix \hat{P}_{i-1} with PAST algorithm, calculating the auxiliary matrix PP need mn^2 operations and the computational complexity from step 2 to 12 in algorithm 1 is $6mnK + O(K)$. Hence, the difference of complexity of SVD and PAST is $O(n^3)$ and $6mnK + O(K)$ respectively, where $m = n$ and $K = 2$ in this simulation. When transmitting antennas increases, the computational complexity of SVD increases by n^3 , which is higher than $12n^2 + O(2)$ of the PAST algorithm. In combination with Fig. 3 and Fig. 4, the proposed PAST-based schemes can achieve near performance with SVD-based hybrid precoding and has lower complexity and less time consumption.

5. Conclusions

In this paper, we propose a low complexity hybrid precoding scheme with HC structure for mmWave massive MIMO system. Firstly, according to a characteristic of block diagonalization of hybrid precoding matrix, the total achievable rate is decomposed into several sub-rates. Then, the optimal unconstrained hybrid precoding matrix of each sub-rate is estimated by the low complexity PAST algorithm. Finally, the analog and digital precoding matrix of sub-rates with constraints are obtained according to the idea of SIC. Simulation results demonstrate that the proposed PAST-based hybrid precoding scheme can achieve similar performance as the SVD-based scheme. And the time consumption and complexity of the proposed PAST-based hybrid precoding scheme are much lower than that of SVD-based scheme with the increase of transmitting antennas.

References

[1] R.W. Heath, N. Gonzalez-Prelcic, S. Rangan, W. Roh, and A.M. Sayeed, "An overview of signal processing techniques for millimeter

wave MIMO systems," *IEEE J. Sel. Topics Signal Process.*, vol.10, no.3, pp.436–453, 2016.

[2] A.L. Swindlehurst, E. Ayanoglu, P. Heydari, and F. Capolino, "Millimeter-wave massive MIMO: The next wireless revolution?," *IEEE Commun. Mag.*, vol.52, no.9, pp.56–62, 2014.

[3] L. Wei, R. Hu, Y. Qian, and G. Wu, "Key elements to enable millimeter wave communications for 5G wireless systems," *IEEE Wireless Commun.*, vol.21, no.6, pp.136–143, 2014.

[4] Y. Wu, C. Xiao, Z. Ding, X. Gao, and S. Jin, "Linear precoding for finite alphabet signaling over MIMOME wiretap channels," *IEEE Trans. Veh. Technol.*, vol.61, no.6, pp.2599–2612, 2012.

[5] J. Mirza, G. Zheng, K.-K. Wong, S. Lambotharan, and L. Hanzo, "On the performance of multiuser MIMO systems relying on full-duplex CSI acquisition," *IEEE Trans. Commun.*, vol.66, no.10, pp.4563–4577, 2018.

[6] S. Han, C.-L. I, Z. Xu, and C. Rowell, "Large-scale antenna systems with hybrid analog and digital beamforming for millimeter wave 5G," *IEEE Commun. Mag.*, vol.53, no.1, pp.186–194, 2015.

[7] S. Sun, T. Rappaport, R. Heath, A. Nix, and S. Rangan, "MIMO for millimeter-wave wireless communications: Beamforming, spatial multiplexing, or both?," *IEEE Commun. Mag.*, vol.52, no.12, pp.100–121, 2014.

[8] O.E. Ayach, S. Rajagopal, S. Abu-Surra, Z. Pi, and R.W. Heath, "Spatially sparse precoding in millimeter wave MIMO systems," *IEEE Trans. Wireless Commun.*, vol.13, no.3, pp.1499–1513, 2014.

[9] X. Yu, J.-C. Shen, J. Zhang, and K.B. Letaief, "Alternating minimization algorithms for hybrid precoding in millimeter wave MIMO systems," *IEEE J. Sel. Topics Signal Process.*, vol.10, no.3, pp.485–500, 2016.

[10] X. Liu, X. Li, S. Cao, Q. Deng, R. Ran, K. Nguyen, and P. Tingrui, "Hybrid precoding for massive mmwave MIMO Systems," *IEEE Access*, vol.7, pp.33577–33586, 2019.

[11] W. Ni, X. Dong, and W. Lu, "Near-optimal hybrid processing for massive MIMO systems via matrix decomposition," *IEEE Trans. Signal Process.*, vol.65, no.15, pp.3922–3933, 2017.

[12] X. Qiao, Y. Zhang, M. Zhou, and L. Yang, "Alternating optimization based hybrid precoding strategies for millimeter wave MIMO systems," *IEEE Access*, vol.8, pp.113078–113089, 2020.

[13] X. Gao, L. Dai, S. Han, C.-L. I, and R.W. Heath, "Energy-efficient hybrid analog and digital precoding for mmWave MIMO systems with large antenna array," *IEEE J. Sel. Areas Commun.*, vol.34, no.4, pp.998–1009, 2016.

[14] Z. Zhang, X. Wu, and D. Liu, "Joint precoding and combining design for hybrid beamforming systems with subconnected structure," *IEEE Syst. J.*, vol.14, no.1, pp.184–195, 2020.

[15] C. Chen, Y. Wang, S. Aïssa, and M. Xia, "Low-complexity hybrid analog and digital precoding for mmWave MIMO systems," *IEEE 31st Annual International Symposium on Personal, Indoor and Mobile Radio Communications*, pp.1–6, 2020.

[16] X. Qiao, Y. Zhang, H. Cao, Z. Xu, and L. Yang, "Hybrid precoders and combiners for sub-connected and fully connected structures," *IEEE International Conference on Consumer Electronics-Taiwan (ICCE-TW)*, pp.1–2, 2019.

[17] H. Zhao and H. Yao, "Design of hybridly-connected hybrid precoding in millimeter-wave massive MIMO system," *Journal on Communications (China)*, vol.41, no.3, pp.45–52, 2020.

[18] D. Zhang, Y. Wang, X. Li, and W. Xiang, "Hybridly connected structure for hybrid beamforming in mmWave massive MIMO systems," *IEEE Trans. Commun.*, vol.66, no.2, pp.662–674, 2017.

[19] Y. Chen, D. Chen, T. Jiang, and L. Hanzo, "Millimeter-wave massive MIMO systems relying on generalized sub-array-connected hybrid precoding," *IEEE Trans. Veh. Technol.*, vol.68, no.9, pp.8940–8950, 2019.

[20] T. Ren and Y. Li, "Hybrid precoding design for energy efficient millimeter-wave massive MIMO systems," *IEEE Trans. Signal Process.*, vol.24, no.3, pp.648–652, 2020.

[21] B. Yang, "Projection approximation subspace tracking," *IEEE Com-*

mun. Lett., vol.43, no.1, pp.95–107, 1995.

Appendix A:

Since $\log_2(|Q_{D-1}|)$ has the same form as Eq. (8), matrix Q_{D-1} can be further decomposed in the similar method, where $Q_{D-1} = I_{N_r} + \frac{\rho}{N_s\sigma^2} HF_{D-1} F_{D-1}^H H^H$. Firstly, denote the matrix F_{D-1} as $F_{D-1} = [F_{D-2} f_{D-1}]$, where F_{D-2} represents the first $D-2$ submatrices and f_{D-1} is the $D-1$ th submatrix. Hence, the matrix Q_{D-1} can be further decomposed:

$$\begin{aligned}
& \log_2(|Q_{D-1}|) + \log_2\left(\left|I_{N_r} + \frac{\rho}{N_s\sigma^2} Q_{D-1}^{-1} H f_D f_D^H H^H\right|\right) \\
&= \log_2\left(\left|I_{N_r} + \frac{\rho}{N_s\sigma^2} H [F_{D-2} f_{D-1}] [F_{D-2} f_{D-1}]^H H^H\right|\right) \\
&\quad + \log_2\left(\left|I_{N_r} + \frac{\rho}{N_s\sigma^2} Q_{D-1}^{-1} H f_D f_D^H H^H\right|\right) \\
&= \log_2\left(\left|I_{N_r} + \frac{\rho}{N_s\sigma^2} (H F_{D-2} F_{D-2}^H H^H + H f_{D-1} f_{D-1}^H H^H)\right|\right) \\
&\quad + \log_2\left(\left|I_{N_r} + \frac{\rho}{N_s\sigma^2} Q_{D-1}^{-1} H f_D f_D^H H^H\right|\right) \\
&= \log_2\left(\left|I_{N_r} + \frac{\rho}{N_s\sigma^2} H F_{D-2} F_{D-2}^H H^H\right|\right) \\
&\quad \left|I_{N_r} + \frac{\frac{\rho}{N_s\sigma^2} H f_{D-1} f_{D-1}^H H^H}{I_{N_r} + \frac{\rho}{N_s\sigma^2} H F_{D-2} F_{D-2}^H H^H}\right|\right) \\
&\quad + \log_2\left(\left|I_{N_r} + \frac{\rho}{N_s\sigma^2} Q_{D-1}^{-1} H f_D f_D^H H^H\right|\right)
\end{aligned} \tag{A.1}$$

The auxiliary matrix $Q_{D-2} = I_{N_r} + \frac{\rho}{N_s\sigma^2} H F_{D-2} F_{D-2}^H H^H$ is also defined, and the above equation can be expressed as:

$$\begin{aligned}
& \log_2(|Q_{D-2}|) + \log_2\left(\left|I_{N_r} + \frac{\rho}{N_s\sigma^2} Q_{D-2}^{-1} H f_{D-1} f_{D-1}^H H^H\right|\right) \\
&\quad + \log_2\left(\left|I_{N_r} + \frac{\rho}{N_s\sigma^2} Q_{D-1}^{-1} H f_D f_D^H H^H\right|\right)
\end{aligned} \tag{A.2}$$

Continue to decompose $\log_2(|Q_{D-2}|)$ in the same way until the total reachable rate formula is completely decomposed, and the following results are obtained:

$$\sum_{i=1}^D \log_2\left(\left|I_{N_r} + \frac{\rho}{N_s\sigma^2} Q_{i-1}^{-1} H f_i f_i^H H^H\right|\right) \tag{A.3}$$

Appendix B:

The proof that optimization problem (13) can be equivalent to (15) is similar to that of Sect. III in [8].

$$\widehat{f}_i^{opt} = \arg \max_{\widehat{f}_i \in \mathbb{F}} \log_2\left(\left|I_K + \frac{\rho}{N_s\sigma^2} \widehat{f}_i^H \widehat{P}_{i-1} \widehat{f}_i\right|\right) \tag{A.4}$$

Firstly, perform singular value decomposition on \widehat{P}_{i-1} , namely, $\widehat{P}_{i-1} = V \Sigma V^H$ and then divide Σ and V into two parts. The above formula can be rewritten as:

$$\begin{aligned}
R &= \log_2\left(\left|I_K + \frac{\rho}{N_s\sigma^2} \widehat{f}_i^H V \Sigma V^H \widehat{f}_i\right|\right) \\
&= \log_2\left(\left|I_K + \frac{\rho}{N_s\sigma^2} \widehat{f}_i^H [V_1 \ V_2] \begin{bmatrix} \Sigma_1 & 0 \\ 0 & \Sigma_2 \end{bmatrix} [V_1 \ V_2]^H \widehat{f}_i\right|\right) \\
&= \log_2\left(\left|I_K + \frac{\rho}{N_s\sigma^2} \widehat{f}_i^H V_1 \Sigma_1 V_1^H \widehat{f}_i + \frac{\rho}{N_s\sigma^2} \widehat{f}_i^H V_2 \Sigma_2 V_2^H \widehat{f}_i\right|\right)
\end{aligned} \tag{A.5}$$

The optimization objective is to find a hybrid precoding matrix \widehat{f}_i which is close enough to matrix V_1 . Hence, \widehat{f}_i and V_2 are approximately orthogonal, i.e. $\widehat{f}_i^H V_2 \approx 0$. According to the principle $I + BA = (I + B)(I - (I + B)^{-1}B(I - A))$, the above formula could be simplified as:

$$\begin{aligned}
R &\approx \log_2\left(\left|I_K + \frac{\rho \Sigma_1}{N_s\sigma^2} \widehat{f}_i^H V_1 V_1^H \widehat{f}_i\right|\right) \\
&= \log_2\left(\left|I_K + \frac{\rho \Sigma_1}{N_s\sigma^2}\right|\right) \\
&\quad + \log_2\left(\left|I_K - \left(I_K + \frac{\rho \Sigma_1}{N_s\sigma^2}\right)^{-1} \frac{\rho}{N_s\sigma^2} (I_K - \widehat{f}_i^H V_1 V_1^H \widehat{f}_i)\right|\right)
\end{aligned} \tag{A.6}$$

Since the eigenvalues of matrix $T = \left(I_K + \frac{\rho \Sigma_1}{N_s\sigma^2}\right)^{-1} \frac{\rho}{N_s\sigma^2} (I_K - \widehat{f}_i^H V_1 V_1^H \widehat{f}_i)$ are small, the approximate formula $\log_2(I_K - T) \approx \log_2(I_K - \text{tr}(T)) \approx -\text{tr}(T)$ can be used to further simplify formula (A.6):

$$\log_2\left(\left|I_K + \frac{\rho \Sigma_1}{N_s\sigma^2}\right|\right) - \text{tr}\left(\left(I_K + \frac{\rho \Sigma_1}{N_s\sigma^2}\right)^{-1} \frac{\rho}{N_s\sigma^2} (I_K - \widehat{f}_i^H V_1 V_1^H \widehat{f}_i)\right) \tag{A.7}$$

According to the high SNR approximation formula $\left(I_K + \frac{\rho \Sigma_1}{N_s\sigma^2}\right)^{-1} \frac{\rho \Sigma_1}{N_s\sigma^2} \approx I_K$, the above formula is simplified as:

$$\begin{aligned}
& \log_2\left(\left|I_K + \frac{\rho \Sigma_1}{N_s\sigma^2}\right|\right) - \text{tr}(I_K - \widehat{f}_i^H V_1 V_1^H \widehat{f}_i) \\
&= \log_2\left(\left|I_K + \frac{\rho \Sigma_1}{N_s\sigma^2}\right|\right) - \left(K - \|\widehat{f}_i\|_F^2\right)
\end{aligned} \tag{A.8}$$

Therefore, maximizing the sub-rate corresponding to the i th subarray is equivalent to maximizing $\|\widehat{f}_i\|_F^2 = \text{tr}(V_1^H \widehat{f}_i)$, which is to minimize the Euclidean distance between the matrix V_1 and \widehat{f}_i . Therefore, optimization problem (13) can be equivalent to the following formula:

$$\widehat{f}_i^{opt} = \arg \min_{\widehat{f}_i \in \mathbb{F}} \|V_K - \widehat{f}_i\|_F^2 \tag{A.9}$$



Rui Jiang was born in Jiangsu, China in 1985. He received the B.S. and Ph.D. degrees in electronic engineering from the Nanjing University of Aeronautics and Astronautics (NUAA), Nanjing, China, in 2007 and 2013, respectively. In 2013 he joined the Department of Telecommunications and Information Engineering, Nanjing University of Posts and Telecommunications (NJUPT), Nanjing, China, where he is now an associate professor. His research focuses on wireless communications.



Xiao Zhou received the B.E. degree in communication engineering from Anhui University of Technology, MaAnShan, China, in 2019. She is currently pursuing the master's degree with the Nanjing University of Posts and Telecommunications (NJUPT), Nanjing, China. Her research interests include high-speed railway communications and beamforming.



Youyun Xu received the Ph.D. degree in information and communication engineering from Shanghai Jiao Tong University (SJ-TU), China, in 1999. He is currently a Professor with the Nanjing University of Posts and Telecommunications. He is also a part-time Professor with the Institute of Wireless Communication Technologies, SJTU. He has over 20-year professional experience of teaching and researching in communication theory and engineering with research and development achievement, such as

the WCDMA Trial System under C3G Framework in China, in 1999, the B3G-TDD Trial System under FuTURE Framework in China, in 2006, and the Chinese Digital TV Broadcasting System. His current research interests include new-generation wireless mobile communication systems (LTE, IM-T Advanced, and related), advanced channel coding and modulation techniques, multiuser information theory and radio resource management, wireless sensor networks, and cognitive radio networks. He is a Senior Member of the Chinese Institute of Electronics.



Li Zhang received the B.S. degree from Changsha University of Science and Technology in 2007, and the M.S. and Ph.D. degrees from Nanjing University of Aeronautics and Astronautics in 2010 and 2015, respectively. He joined the College of Computer Science and Technology of Nanjing Forestry University as a Lecturer in 2016. His current research interests include machine learning and high-speed railway communications.